A Hybrid Technique for System-Level Signal Integrity and EMC Assessment

A Hybrid Technique for System-Level Signal Integrity and EMC Assessment

S. Grivet-Talocia, I. S. Stievano, I. A. Maio, F. G. Canavero

Dip. Elettronica, Politecnico di Torino, C. Duca degli Abruzzi 24, 10129 Torino, Italy
Ph. +39 011 5644060, Fax +39 011 5644099 (e-mail canavero@polito.it)

Abstract

This paper presents a hybrid technique for the system-level assessment of Signal Integrity and Electromagnetic Compatibility of digital electronic systems. We describe a stable procedure for the inclusion of behavioral models of digital drivers and receivers into a Finite-Difference Time-Domain mesh. The behavioral models for the devices are based on Radial Basis Function (RBF) formulations, allowing for inclusion of intrinsic nonlinear and dynamic effects. The particular adopted formulation allows us to apply the hybrid method to investigate both interference from incident fields and radiation for interconnected structures loaded by realistic drivers and receivers.

1 Introduction

The high complexity of modern electronic systems requires careful modeling strategies at early stages of the design process. This is particularly important for the characterization of interconnected structures loaded by digital drivers and receivers. Indeed, it is well known that Electromagnetic Compatibility (EMC) and Signal Integrity (SI) are strongly affected by the geometry of the interconnects and by the possibly complex nonlinear/dynamic behavior of the electronic devices collocated at their terminations. For a reliable design, predictions combining a rigorous full-wave scheme together with precise models of digital ports are needed. Strong nonlinearities and dynamic behavior of digital devices are correctly represented by a detailed transistor-level circuit, which is however too heavy to be considered for direct inclusion within a full-wave modeling tool. Moreover, such a description is most often unavailable, since it may possibly disclose intellectual property information.

This paper presents a hybrid technique combining the flexibility of Finite-Difference Time-Domain (FDTD) schemes for full-wave solution of complex structures with the accuracy and efficiency of behavioral models for digital ports based on Radial Basis Functions (RBF) expansions [9]. Such models allow the description of digital drivers and receivers as discrete-time nonlinear dynamic parametric macromodels, which lead to a virtually undistinguishable response under very different loading conditions with respect to the full transistor-level model of the device. There are two main advantages in this strategy. First, no knowledge of transistor-level circuit is required, since the behavioral model can be obtained through a standard identification process by considering the device as a black-box. Second, the computational cost required for the simulation of a behavioral model is much less than for the corresponding transistor-level model.

Behavioral models are inserted as lumped elements within the FDTD computational mesh through a standard procedure [10]. However, care must be taken since both FDTD and RBF models are discrete-time systems with a possible different sampling time. In order to overcome this problem, we have devised a time resampling strategy for RBF models which is capable of preserving both time stability and accuracy. As a result, a stable nonlinear full-wave solver is obtained, including very accurate models of real-world drivers and receivers. This solver, based on a scattered field formulation of the FDTD equations, allows investigation of both interference from external fields and radiation prediction for interconnection structures loaded by accurate models of digital drivers and receivers.

The following sections give some detail on RBF macromodels, on time resampling issues, and on the FDTD hybridization. Finally, numerical results will be presented.

2 RBF macromodels

Let us consider a single digital driver or receiver with port voltage and current denoted as $v(t)$ and $i(t)$, respectively. The actual dynamic behavior of the device requires an appropriate sampling time T_s for the characterization of any possible voltage and current waveform. For instance, this sampling time should be significantly smaller than the fastest rise time allowed by the specific technology. We indicate the voltage and current samples at the port of the device under modeling as

$$v^m = v(mT_s)\,, \qquad i^m = i(mT_s)\,, \tag{1}$$

A general form of parametric macromodel can be expressed as [5, 8]

$$i^m = F(\Theta; \mathbf{x}_i^{m-1}, v^m, \mathbf{x}_v^{m-1}; m)\,, \tag{2}$$

where $\mathbf{x}_v^{m-1}$ and $\mathbf{x}_i^{m-1}$ are regressor vectors collecting the past r voltage and current samples,

$$\begin{aligned} \mathbf{x}_v^{m-1} &= \left[v^{m-1}, v^{m-2}, \ldots, v^{m-r}\right]^T, \\ \mathbf{x}_i^{m-1} &= \left[i^{m-1}, i^{m-2}, \ldots, i^{m-r}\right]^T. \end{aligned}$$

These vectors act as discrete-time internal states of the model, with r indicating its dynamic order. The function F is a nonlinear mapping from $\Re^{2r+1}$ to $\Re$ defining the *model representation* and Θ is the vector of model parameters, defining the *model structure*. Note that F depends also on time m, since digital drivers must be modeled as time-varying components in order to capture switching behavior.

In this work we mainly concentrate on model representations F defined by Gaussian Radial Basis Function (RBF) expansions [2, 4, 8]. Such representations provide approximations of the mapping F through expansion into L multivariate Gaussian functions of suitable width β centered at appropriate points $\mathbf{c}$ in the regressor space of dimension $2r+1$. A general form of such representation can be expressed by

$$F(\Theta, \mathbf{x}_i^{m-1}, v^m, \mathbf{x}_v^{m-1}) = \sum_{l=1}^{L} \theta_l \, \Psi_l(m-1) \, \exp\left\{-\frac{(v^m - c_l^0)^2}{2\beta^2}\right\}$$

where the term $\Psi_l(m-1)$ collects all contributions due to past voltage and current samples,

$$\Psi_l(m-1) = \exp\left\{-\frac{||\mathbf{x}_i^{m-1} - \mathbf{c}_l^i||^2 + ||\mathbf{x}_v^{m-1} - \mathbf{c}_l^v||^2}{2\beta^2}\right\}$$

and $||\cdot||$ denotes the Euclidean norm.

The RBF representations can be applied to a wide range of modeling problems, as they lead to general results on the existence on nonlinear parametric models [6, 7]. They are numerically efficient (the evaluation of an expansion term requires the evaluation of norms in the multidimensional regressor space plus scalar functions) and the estimation of their parameters is easier than for other representations [2, 4]. Besides, the Gaussian RBF have local support. This feature further simplifies the parameter estimation and leads to asymptotically vanishing models. From a practical point of view, Gaussian RBF representations are well suited for digital I/O ports, as they can produce a model meeting the accuracy and efficiency specification of real simulation problems, at a low modeling cost.

The following two sections particularize the general form of RBF model to digital output ports (drivers) and input ports (receivers).

2.1 Drivers

One of the main difficulties in macromodeling output ports of drivers arises from the time-varying nature of the devices due to switching. Our proposed strategy amounts to using two separate Gaussian RBF submodels accounting for both static and dynamic effects of the port behavior at a fixed logic state, henceforth labeled i_u^m for HIGH and i_d^m for LOW state. These two submodels are time-invariant. A piecewise linear combination through time-varying weight functions $w_{u,d}^m$ provides a model for the evolution of the port logic state, acting as a switch between submodels $i_{u,d}^m$. A more detailed discussion on the systematic derivation of the model together with guidelines for the estimation of its parameters can be found in [9].

2.2 Receivers

Macromodeling of receivers input ports follows a similar approach to that used for drivers. However, receivers are not time-varying components, therefore simpler models can be devised. The proposed structure for a receiver model is

$$i^m = i_{\text{lin}}^m + i_{\text{nl},u}^m + i_{\text{nl},d}^m \tag{3}$$

where i_{lin}^m is a linear parametric submodel accounting for the mainly linear behavior of the port for voltage values within the range of the power supply voltage, while $i_{\text{nl},u}^m$ and $i_{\text{nl},d}^m$ are Gaussian RBF submodels taking into account both the nonlinear static and dynamic effects of the up and the down protection circuits, respectively.

3 Resampling of RBF macromodels

In Section 2 we presented the general form of a discrete-time parametric model (see Eq. 2) that can be applied for an effective behavioral description of fast digital drivers and receivers. One of the key parameters of such model is the sampling time T_s used in the identification stage. The model dynamic equations strongly depend on this sampling time, since the internal states $\{\mathbf{x}_v, \mathbf{x}_i\}$ collect past samples of voltages and currents delayed by multiples of T_s. The numerical simulation of the model equations appears then to be constrained to use this sampling time. However, if this model is to be combined with an FDTD code as a lumped element, some problems might occur due to the Courant condition, which limits the time step Δt to a maximum value depending on the spatial dimensions of

the FDTD cells. This section briefly describes the resampling procedure to be applied to the parameteric model (2) in order to match its sampling time to the one determined by the FDTD mesh. Details on the derivation and on the appropriate stability analysis can be found in [3].

Resampling can be viewed as a two-step process. First, the discrete-time model is converted into a continuous-time model. Then, a suitable time discretization scheme is applied to get a resampled model. Conversion of Eq. (2) to continuous time requires the derivation of a system of state equations with appropriate dynamic order. Since r past samples of both voltage and current are involved in the discrete-time equations (see Eq. 3), we use a global dynamic order $2r$ also for the continuous-time model. The continuous state variables will be delayed voltages and currents. A continuous time state equation is easily derived by using a first-order forward approximation of the time derivative

$$\frac{\mathbf{x}^{m+1} - \mathbf{x}^m}{T_s} \sim \left.\frac{d\mathbf{x}}{dt}\right|_{t=mT_s} \tag{4}$$

and replacing differences of discrete samples with time derivatives of the corresponding continuous state variables at time mT_s. The leading error term in this approximation is $O(T_s^2)$.

The resulting continuous-time state equation is discretized using the same forward approximation of the time derivative but using the new (FDTD-related) sampling time Δt. Henceforth we will indicate with

$$\tau = \frac{\Delta t}{T_s} \tag{5}$$

the resampling factor. We remark that due to the employed forward difference approximation of the time derivative, the system of resampled state equations can be split into an explicit part of linear update equations plus an implicit nonlinear output equation, which is not dynamic. This output equation depends also on the re-discretized delayed state variables, but it has the same form as Eq. 2, being a discrete-time relation between voltage and current samples with sampling time Δt.

4 FDTD and lumped elements

We describe here the adopted procedure for the insertion of resampled RBF macromodels in a FDTD mesh. In this paper we adopt a scattered field formulation of Maxwell equations, in order to allow for incident field interference on a given structure. The resulting form of Ampere-Maxwell curl equation to be discretized via FDTD is therefore

$$\nabla \times \mathbf{H}_s + \varepsilon_0 \frac{\partial \mathbf{E}_i}{\partial t} = \varepsilon \frac{\partial \mathbf{E}}{\partial t} + \sigma \mathbf{E} + \mathbf{J}\,, \tag{6}$$

where the subscripts i and s denote incident and scattered field, respectively. The entire computational domain surrounding the structure under investigation is discretized with a FDTD mesh with size Δx, Δy, Δz along the three Cartesian coordinates.

Let us consider now the collocation of a generic lumped element in the $\{i, j, k\}$ cell along the $\hat{z}$ coordinate. The current density $\mathbf{J}$ associated with the lumped element can be expressed in terms of the current I_L as

$$\mathbf{J} = \frac{I_L}{\Delta x \Delta y}\,\hat{z}\,, \tag{7}$$

while the lumped voltage V_L is expressed in terms of the total electric field through integration over one cell edge

$$V_L = \int \mathbf{E} \cdot \hat{z}\, dz\,. \tag{8}$$

The collocation of the lumped element in the FDTD mesh amounts to combining Eqs. (6), (7) and (8). This is a standard procedure and is not detailed here. Further details can be found in [3, 10]. In summary, the insertion of a RBF macromodel into an FDTD mesh leads to the following modifications to the basic update equations

- A set of $2r$ linear state equations is required for the time update of the internal states of the RBF macromodel. These equations are intrinsically discrete-time and are fully explicit.
- A system of (static) nonlinear equations is required for the update of voltage and current at the device port once the internal states have been computed. This syetem is solved by means of a Newton-Raphson technique at each time iteration. The numerical experiments that we performed using RBF models for commercial drivers and receivers converged at any time iteration in less than 3 Newton-Raphson iterations with a relative error smaller than 10^{-9}.

5 Examples

We first show a validation of the hybrid technique on a controlled structure for which several simulation approaches can be adopted. The structure that we chose for validation is a simple transmission line in free space made of two equal conducting strips (115.68mm × 2.89mm) separated by 2.17mm. The effective characteristic impedance of the resulting transmission line is $Z_c \sim 131\,\Omega$, while the line delay is $T_D \sim 0.4$ ns. The line is terminated at the near end by the lumped RBF macromodel of a commercial driver. The driver forces a bit pattern `'010'` at its output port, with a bit time of 2 ns. The far end termination is a shunt connection of a 1 pF capacitor and a 500 Ω resistor.

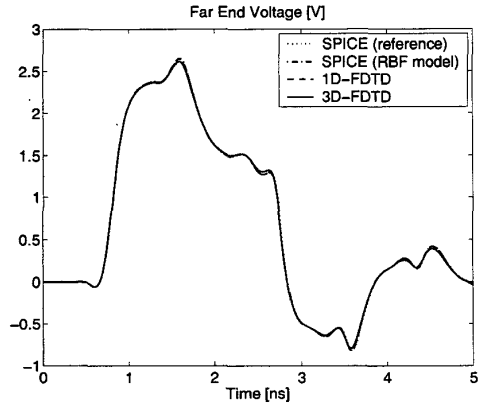

Figure 1: Far end termination voltages with switching driver at near end and capacitive load at far end. See text for additional details.

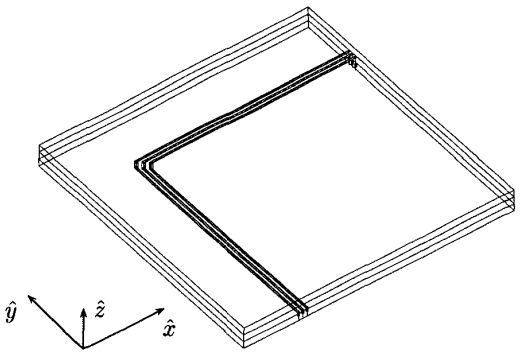

Figure 2: PCB structure for illustration of incident field coupling.

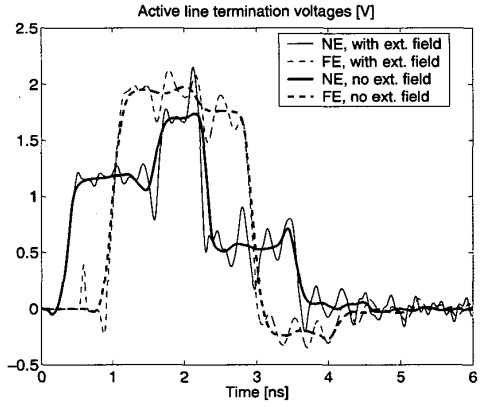

Figure 3: Termination voltages with and without incident field contribution (NE, near end; FE, far end).

The simulation results are depicted in Fig. 1, where four different curves are plotted for the far end voltage. The first curve is the result of a SPICE simulation using the transistor-level model of the driver. This can be regarded as the reference curve. The second curve is obtained always with SPICE but using the RBF model of the driver. This can be regarded as a validation for step 1 above. The third curve is the result of a FDTD simulation of the (one-dimensional) telegraphers equations using the RBF model. This curve is intended to validate the FDTD implementation, the resampling strategy, and the iterative nonlinear solver without the influence of spurious numerical dispersion occurring in three-dimensional FDTD. Finally, the fourth curve shows the result of the full-wave simulation. The latter was performed with the maximum allowed time step $\Delta t \sim 1.39$ ps. Since the sampling time used for identification of the RBF model was $T_s = 10$ ps, the resulting resampling factor is $\tau = 0.139$. As expected, the four curves are almost undistinguishable. Only the 3D-FDTD result has a marginal deviation from the other curves due to numerical dispersion.

The hybrid nonlinear full-wave solver is applied next to assess SI and EMI/EMC of board-level interconnected systems terminated by drivers and receivers. As an example, we consider the 5 cm $\times$ 5 cm PCB structure depicted in Fig. 2. Three 400 μm-wide coupled strips run parallel to each other on the top (along x coordinate, length 4 cm) and bottom (along y coordinate, length 4 cm) of the PCB signal layer. Three vias connect the orthogonal sections of the strips. Top and bottom glue layers cover the signal layer, and the entire PCB is metallized on both sides. The innermost strip is driven by the RBF macromodel of a driver on one end and is terminated on the other end by the RBF macromodel of a receiver. All the other terminations consist of 50 Ω resistors. The driver forces a `'010'` bit sequence at its output port. In addition, an external wave pulse impinges on the structure from a direction $\{\theta = 90^o, \varphi = 180^o\}$ with θ-polarized electric field in standard spherical coordinates. The amplitude of the pulse is 2kV/m, with a bandwidth of 9.2 GHz. Fig. 3 shows the termination voltages for the driven line with and without incident field. This example illustrates that the proposed modeling strategy can be employed for the complex task of predicting incident-field coupling effects on interconnected networks loaded by real-world components.

The proposed technique can also be applied for system-level EMC assessment and for radiation analysis in presence of nonlinear terminations. Indeed, it is well-known that radiated fields predictions may be strongly biased if the employed models of drivers and receivers are too simple [1]. As an example, we consider the same structure above but without incident field interference. The only excitation is therefore the pulse forced by the driver. Since this structure is shielded on top and bottom by two conducting layers, the far-field radiated fields can be easily

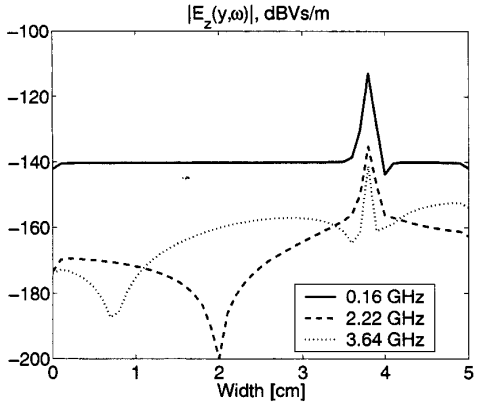

Figure 4: Near field $|E_z(y,\omega)|$ along one of the board edges at various frequencies.

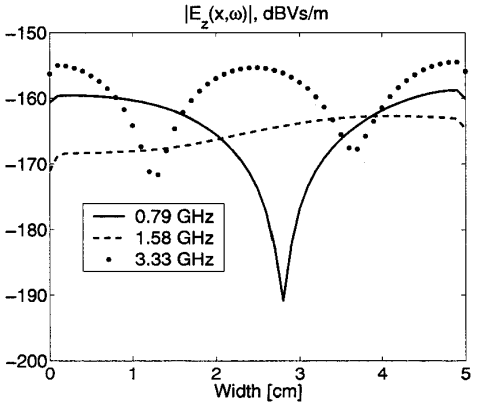

Figure 5: Near field $|E_z(x,\omega)|$ along one of the board edges at various frequencies.

computed from the frequency-domain tangential electric and magnetic fields at the board edges. The magnitude of such fields is therefore a good observable to be analyzed in order to characterize radiation. Frequency-domain field components can be computed by using standard Fourier transform of the corresponding time-domain waveforms. It should be noted that the latter are computed using the full nonlinear driver and receiver models. We report in Fig. 4 the spatial distribution along one of the board edges ($[x,z]$ fixed, closest edge to far end terminations of the three strips) of the field component $|E_z(y;\omega)|$. This distribution is computed at different frequencies in order to show possibly resonant behaviors. The signature of the TEM mode due to signal propagation along the strips is clearly visible in the plots. Figure 5 shows instead the field distribution at various frequencies along the x direction for the board edge with $[y,z]$ fixed, far from the driver. Computation of far fields from selected field components is a standard task [10].

Conclusions

A hybrid technique for the full-wave modeling of interconnected systems with nonlinear/dynamic terminations has been presented. The digital devices are represented via their RBF-based behavioral macromodels, which have been proved to reproduce closely their actual port behavior under very different loading conditions. A suitable resampling strategy, allowing for the conversion of RBF macromodels into a form that can be directly plugged in a FDTD solver, has been described. The resulting nonlinear field solver has been applied to characterization of signal integrity, electromagnetic interference, and radiation for PCB structures.

References

[1] F. Canavero, S. Grivet-Talocia, I. Maio, and I. Stievano, "Numerical modeling of digital devices' impact on EMC/EMI," in *2001 IEEE EMC International Symposium, Montreal, Canada*, pp. 582–587, August 13–17, 2001.

[2] S. Chen, C. F. N. Cowan and P. M. Grant, "Ortogonal least squares learning algorithm for radial basis function network," *IEEE Transactions on Neural Networks*, Vol. 2, No. 2, pp. 302–309, Mar. 1991.

[3] S. Grivet-Talocia, I. S. Stievano, F. G. Canavero, "Hybridization of FDTD and Device Behavioral-Modeling Techniques", *IEEE Trans. EMC*, in press.

[4] K. Judd and A. Mees, "On selecting models for nonlinear time series," *Physica D*, Vol. 82, pp. 426–444, 1995.

[5] L. Ljung, *System identification: theory for the user,* Prentice-Hall, 1987.

[6] I. W. Sandberg, "Approximations for nonlinear functionals," *IEEE Transactions on Circuits and Systems I*, Vol. 39, pp. 65–67, Jan. 1992.

[7] I. W. Sandberg, "Approximation theorems for Discrete-Time Systems," *IEEE Transactions on Circuits and Systems*, Vol. 38, pp. 564–566, May 1991.

[8] J. Sjöberg et al., "Nonlinear black-box modeling in system identification: a unified overview," *Automatica*, Vol. 31, No. 12, pp. 1691–1724, 1995.

[9] I. S. Stievano, F. G. Canavero, I. A. Maio, "Parametric Macromodels of Digital I/O Ports," *IEEE Trans. Advanced Packaging*, May 2002, in press.

[10] A. Taflove (ed.), *Advances in Computational Electrodynamics: The Finite-Difference Time-Domain Method*, Norwood, MA: Artech House, 1998.